TURBULENT FLOW STRUCTURE IN FULLY DEVELOPED NARROW RIB-ROUGHENED CHANNEL WITH PIV TECHNIQUE

Md. Shafiqul Islam and M. Monde*
Saga University, Saga 840 -8502, Japan
K. Haga, M. Kaminaga and R. Hino
Japan Atomic Energy Research Institute, Tokai 319-1195, Japan

Abstract An experimental study has been carried out to investigate turbulent flow pattern over one side micro-repeated-ribs in two-dimensional narrow rectangular channel by particle image velocimetry (PIV) technique with water as working fluid. Two micro-rib-pitch-to-height ratios (p/k) were 10 and 20 while holding the rib height constant at 4 mm. The rib height-to-channel equivalent diameter ratio (k/D_e) is 0.1. The instantaneous vector data were taken in the fully developed flow region (x/D_e =18) for Reynolds number ($Re = u D_e / \nu$) ranging from 1,400 to 50,000 by using a cross-correlation technique. The local velocity fields in the cross-section of the flow channel were measured in the upstream, on the rib-tip, and in the downstream regions, respectively and the turbulent kinetic energy ($\kappa = 1/2 (u_{rms}^2 + v_{rms}^2)$) fields were, then, calculated for the same regions. Reattachment length was measured from velocity vector map. The effect of the p/k ratio and the Re on the reattachment length was investigated. The results showed that the p/k ratio and the Reynolds number have no significant effect on the reattachment length and its value is approximately 4 times the rib height.

Keywords Turbulent flow pattern, Micro-repeated-rib, Narrow channel, PIV

1. INTRODUCTION

Strongly separated and recirculated flows over micro-repeated-ribs in turbulent water flows have recently become the center of intensive investigation. Despite their frequent appearance in engineering arena, their experimental and theoretical studies are rather limited due to the difficulties encountered in the investigations. This is mainly because turbulent flows over ribs create crossover flow, strong eddy, separation, and reattachment and the physics of flow in the recirculation zone is the complex in nature. In addition to these, two basic engineering flows, i.e, forward and backstep flows that also occur downstream of the ribs to the reattachment point. A basic characteristic of such flow configurations is the integral parameter of the length of the reattachment (L_R) behind the rib. This length depends on the ratio of the boundary layer thickness of the approaching flow to the rib height and also on the geometry of the rib itself .In order to understand the physical mechanism ofsuch a complex turbulent flow pattern, it is necessary to obtain instantaneous velocities over the entire flow field. Particle image velocitmetry (PIV), which is a well-developed technique, has been widely used for various turbulent measurements with reasonable accuracy and reliability. This has made flow-pattern analysis an important aspect of many investigations. In a typical PIV experiment, small tracer particles are illuminated by a double-pulsed laser sheet of light, and the images of these particles are captured using either a CCD camera or photographic film. Then, instantaneous velocity fields of 2D or 3D are determined by analyzing displacements of these particle images using a correlation technique. If the depth-of-focus of the camera is made larger than the thickness of the laser sheet, all of the illuminated particles are in focus in the recorded image. Flow over a two-dimensional surface roughness of this type is of interest in augmenting heat transfer for high heat flux removal, for example, spallation target system design (Shafiqul et al. (1998)). There are no experimental and analytical results available on a very narrow rectangular channel with micro-repeated-ribs under water-flow conditions. Most of the experimental and analytical studies have been conducted on surface roughness under air-flow conditions.

Bradshaw and Wong (1972) studied the low-speed flow downstream of steps and fences by a cross-wire probe and a constant-temperature anemometers methods with a rectangular cross sectional shape. They reported that for a single roughness element, the flow was reattaching approximately 6 step heights downstream from the step. Bergeles and Athanassiadis (1983) studied on the flow field past a surface mounted obstacle with obstacle width (w) to height (k) ratios (w/k) 1 to 10 by a single hot wire method. They predicted the dependency of the length of recirculating region on the

*Email:monde@me.saga-u.ac.jp

obstacle widths in the upstream and downstream regions. The reattachment length strongly depends on obstacle width for w/k less than 5 and it increases sharply with the decrease of obstacle widths. However, the reattachment length remains constant for w/k >5 and equals to 3 times the obstacle height. Logan and Phataraphruk (1989) studied the response of a turbulent pipe flow to a single roughness element by a single hot wire method.Their geometrical configuration was roughness width (w) to height (k) ratios (w/k) 0.35 to 2.1 and roughness height (k) to pipe radius (R) ratios (k/R) 0.1 to 0.3. Their findings agree qualitatively with that of Bergeles and Athanassiadis. Faramarzi and Logan (1990) also reported the same observation with that of Bergeles and Athanassiadis and Logan and Phataraphruk for a single roughness element with the ratios of w/k 1 to 7 and the ratios of k/R 0.1 to 0.2. Mantle (1966) investigated the effect of p/k on the reattachment length for square ribs (w/k =1). He reported that the reattachment length does not occur for p/k less than 6.6 and that for p/k between 6.6 and 12, the reattachment length remains constant and its value is 4 times the rib height. His value of L_R/k increase from 4 to 8.5 as p/k increases from 12 to 28 and remains constant at 8.5 for p/k larger than 28. Whereas Faramarzi and Logan reported a value of $L_R/k = 9.1$ for a square rib of infinity p/k. Most of the studies have been experimentally done to understand the flow phenomena associated with flows past two-dimensional ribs.

A pretty number of numerical studies were conducted by Durst and Rastogi (1980), Acharya et al. (1994), Chang and Mills (1993), Lee and Abdel-Moneim (2001) with single or two or repeated roughness elements as to predict the flow behavior in flows past two-dimensional ribs. All of their investigations are based on air-flow conditions for a large roughness geometry configuration. Until now, to the authors' knowledge, turbulent water flow measurement experiments by PIV or analytical study over one side micro-repeated-ribs in two-dimensional narrow channel have not been carried out yet. Therefore, this paper experimentally presents various turbulent water flow patterns that occur over one side micro-repeated-ribs in two-dimensional narrow channel by particle image velocimetry (PIV) technique. The rib-pitch-to-height ratios (p/k) are 10 and 20. The rib height-to-channel equivalent diameter ratio (k/D_e) is 0.1.

2. EXPERIMENTAL PROGRAM

2.1 TEST APPARATUS

The schematic diagram of experimental set-up and data acquisition system is shown in **Fig.1**. The closed-loop system incorporates a test section, a pair of Nd: YAG laser, a CCD camera, a PIV 2000 processor, a PC, a water tank, and a water pump etc. Small tracer particles were seeded into the flow. Throughout the measurements, it was assumed that the tracer particles were homogeneously distributed over the whole viewing volume, including those regions close to the wall. Working fluid (water) from the pump was supplied to the test section through the flow meters, and then, it passed through a filter, a cooler, the water tank and to the pump again. The filter was used to filter out the solid particles,which were larger than the seeding particles size that may have found their way into the system. The cooler was employed to control the temperature of the water in the test section. The water tank served as a container into which water from the test section was discharged, conditioned, and recirculated. The flow rate through the test section was measured using two electromagnetic flow meters in parallel and was controlled by pumping power with an inverter. Inlet and outlet temperatures and pressures were recorded by a data acquisition system. Two differential pressure taps were installed to measure the static pressure drop across the test section and the distance between the two pressure taps was 1,100 mm. The measurement was carried out at a location of about $x/D_e = 18$ to ensure the fully developed flow region where x is the length from channel inlet to measurement zone, and D_e is the channel equivalent diameter.

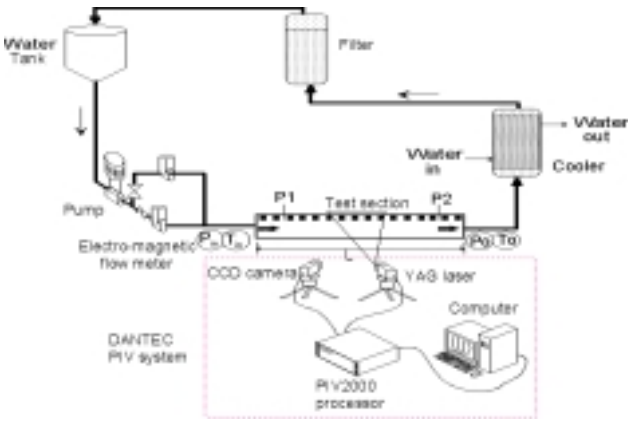

Fig. 1 Schematic diagram of experimental apparatus for PIV

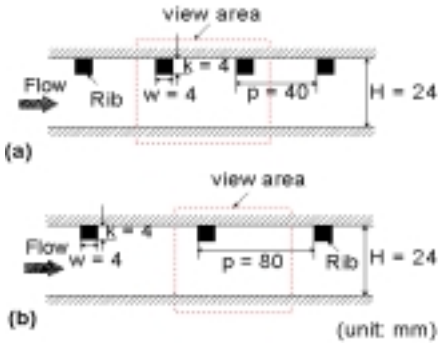

Fig. 2 Cross section of flow channel along with view area (a) p/k = 10 (b) p/k = 20

Fig. 2 shows the longitudinal cross section of the flow channel of the two test sections and their major parameters. Camera view area was also shown as to clear about the flow measurement regions of the two

roughness geometries (p/k = 10, 20). The test section was 1,450 mm in length, 120 mm in width, and 24 mm in height. Square rib, whose cross-sectional dimension is 4 mm × 4 mm, was employed throughout the entire flow length of the test section as they reveal the better heat transfer performance than that of the triangular or semicircular ribs.

The flow does not travel smoothly over the square ribs and the square cross-sectional blockage accentuates inertial losses. A detailed description of the PIV measurement system has been given to the following section.

2.2 PIV MEASUREMENTS

The whole PIV measurement step is as follows: (1) construction of water flow channel, (2) seeding of tracer particles, (3) visualization and capturing images, (4) calculation of 2-D velocity vectors, and (5) post-processing for analyses. After construction of the water flows to be measured, tracer particles of 10 μm in size were seeded into the flows and were illuminated with the double-pulsed Nd:YAG laser at a frequency of 15 Hz and power of 150 mJ / pulse. A CCD camera of 1K × 1K pixels resolution was used to capture PIV images. The viewing direction of the camera is normal to the plane of the light sheet. The vector field of the flow velocity within the plane of the light sheet can then be determined forming the displacement between the image of the tracer particles and the delay time between the two laser pulses. The time interval between the two laser pulses can be adjustable depending upon the flow velocity and the spatial resolution of images in the experiment. A PIV 2000 processor of Dantec Dynamics A/S is optimized for processing the PIV images into a raw vector map in near real time and transferring this to be stored (recorded) in the database of the PC. This processor calculates velocity vectors by cross correlation algorithm technique. This correlation can then be carried out through the Fast Fourier Transforms (FFTs). The image map is divided into FFT interrogation areas of rectangular shape whose size is 16 × 16 that are expressed as a number of pixels. The double-pulsed Nd:YAG laser and the CCD camera were connected to work station (host computer, RAM 456 MB, HDD 4 GB) via a synchronizer, which controlled the timings of two laser illuminations and CCD camera image capturing. The experimental conditions and their parameters are given in **Table 1**.

Table 1 Experimental parameters

General properties	
System	Deionized water
Temperature	287 K
Reynolds number	1,400 to 50,000
Seeding	
Product	Expancel (461DU)
Mean diameter	≈10 μ m
Density	1.3 kg /m^3
PIV imaging	
Image size	[1008 × 1018] pixels
Object size(p/k = 10)	[52.5 × 53]mm
Object size(p/k = 20)	[66.2×67]mm
Time interval between pulses	[150 to 1,300] μ s
Nd: YAG PIV laser	
Wave length	532 nm
Power	150 mJ / pulse
Pulse width	10 ns
Light pulses per recording	2
Light sheet thickness	≈1mm
CCD camera	
Light cell pixels	[1008 × 1018] pixels
Frame mode	Double
Time between two frames	1 μ s
Frame rate	15 pair/s
PIV interrogation algorithm	Cross correlation
Interrogation resolution	[16×16] pixels

3. RESULTS AND DISCUSSION

The instantaneous vector data were taken in the fully developed flow region (x/D$_e$ = 18) for the Reynolds num-

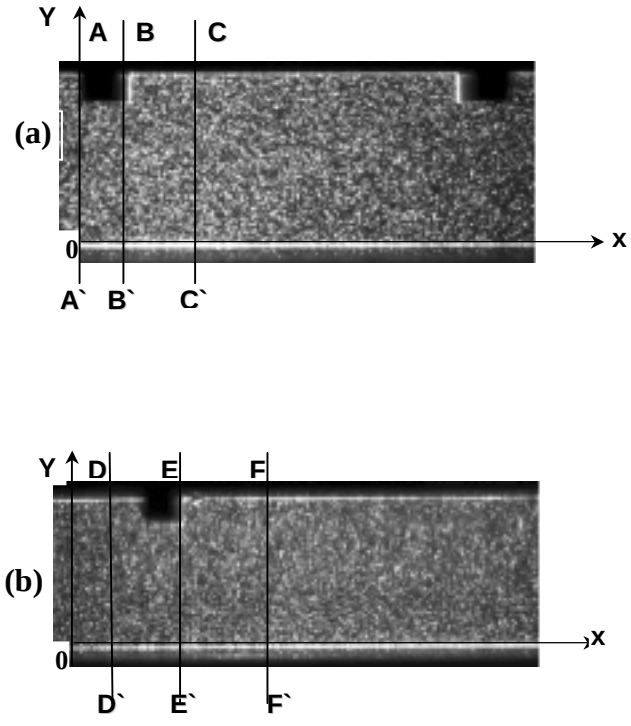

Fig. 3 Visualized field with seeding particles
(a) p/k = 10 (b) p/k = 20

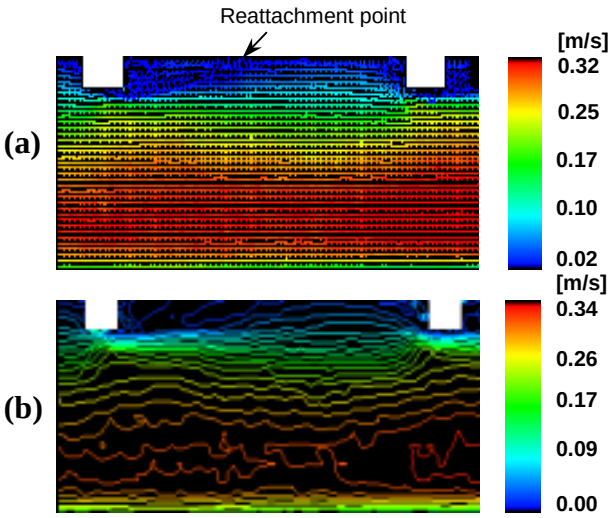

Fig. 4 Velocity contour map at Re = 7,000
(a) p/k = 10 (b) p/k = 20

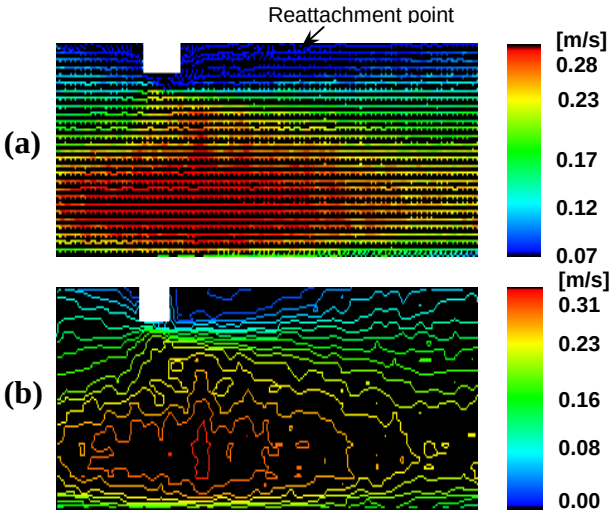

Fig. 5 Velocity contour map at Re = 7,000
(a) p/k = 10 (b) p/k = 20

ber (Re) ranging from 1,400 to 50,000 by using a cross-correlation technique. A total of 83×84 = 6,972 PIV vector data were obtained for each flow case. The resolution of each local velocity field data was either 0.6 or 0.7 mm in the X and Y directions. **Fig. 3** shows the image maps with seeding particles within the field of view at p/k = 10 and 20, respectively. **Fig. 4** shows the velocity field and its contour map at p/k = 10 for Re = 7,000.The velocity contour map was formed by combining the two components of local velocity so as to comprehend the local velocity magnitude at different locations of the flow channel. The local velocity distributions and magnitudes are shown by five color levels; red, yellow, light green, light, and deep blue in the legend bar located at the right side of each vector and

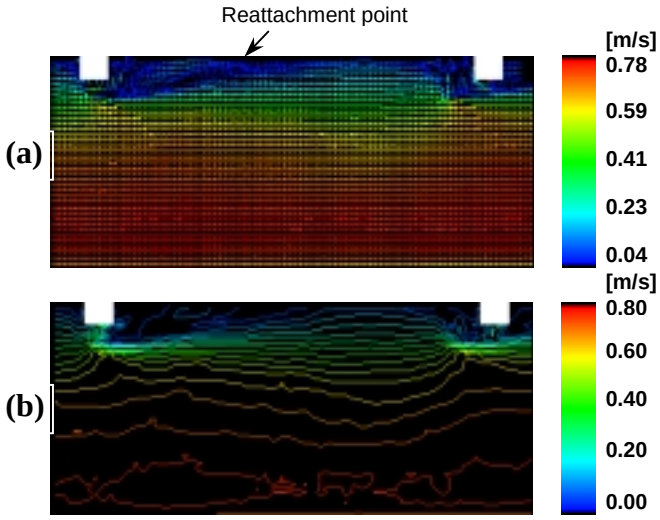

Fig. 6 Velocity contour map at Re = 20,000
(a) p/k = 10 (b) p/k = 20

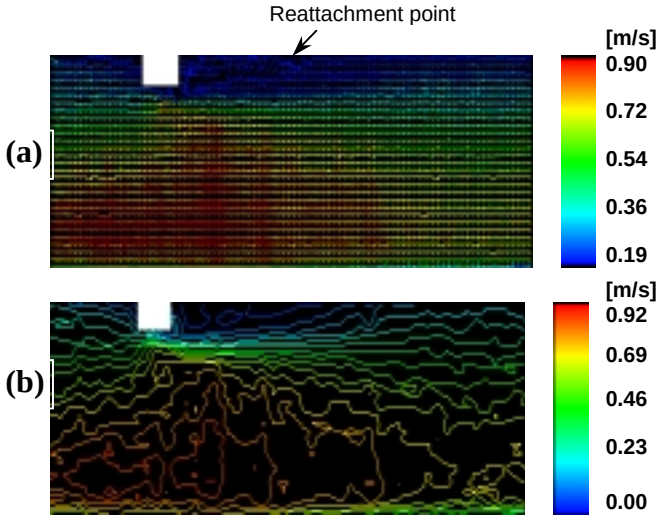

Fig. 7 Velocity contour map at Re = 20,000
(a) p/k =10 (b) p/k = 20

contour map. It is seen from **Fig. 4** that the ribs produced strong turbulence that caused recirculation, separated, and or reattaching flows downstream of the ribs. The local velocity is very low in the recirculation zone, which is about 0.02 m/s. The maximum local velocity was observed below the mid-position of the flow cross-sectional area, which is shown as a red color in the legend bar. Streamwise local velocity distribution just above the smooth wall was not varied a lot compared with the uniform inlet velocity of 0.2 m/s. However, the local velocity changes dramatically due to the presence of ribs at the opposite wall. Strong secondary flows and corner eddies were also observed in the inter-rib regions in the contour map. One can clearly identify the locations where the separated flow reattaches to the wall. The reattachment points were

more accurately determined from the rearward tip of the rib to the x-velocity reverses from a positive to a negative value. The measured reattachment length is 12 mm long from the rearward tip of the rib at Re =7,000 and p/k = 10.

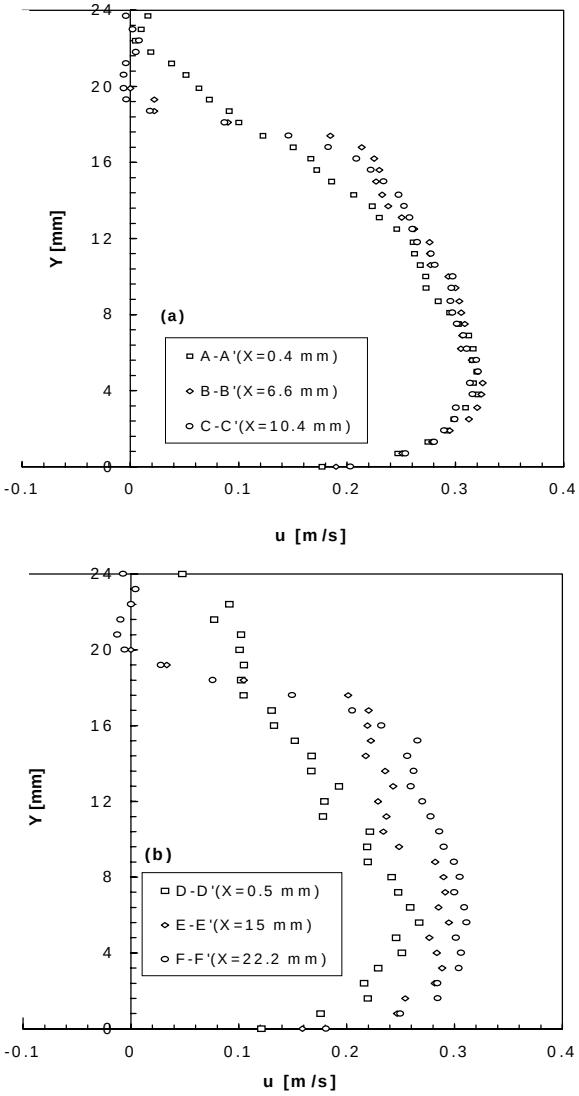

Fig. 8 Streamwise velocity profiles at Re = 7,000
(a) p/k = 10 (b) p/k = 20 **Fig. 5** shows the velocity field and its contour map at the same Re but at p/k = 20. The reattachment occurs at a distance of 15 mm from the rearward tip of the rib at Re = 7,000. For this rib geometry, the reattachment length has been augmented by 3 mm longer than the previous rib geometry (p/k = 10). This is because of its two-fold wider rib pitch. **Fig. 6** also shows the velocity field and its contour map as to see the effect of high Re on the reattachment length at the same rib geometry. The results showed that the reattachment length increases slightly for high Re and p/k = 10. **Fig. 7** shows the velocity field and its contour map as to see the effect of high Re on the reattachment length at a wider rib pitch. The results also showed that the reattachment length decreases slightly for high Re and p/k =20.These trends can be considered due to some measurement uncertainties. **Figs. 8** and **9** show the streamwise velocity profiles in the upstream (A-A`, D-D`), on the rib-tip (B-B`, E-E`) and in the downstream (C-C`, F-F`) regions over the cross-section of the flow channel at Re=7,000 and 20,000, respectively. The aforementioned symbols were shown on the image maps. The velocity profiles and then, the turbulent kinetic energy profiles were calculated along those cross sectional areas of the flow channel. The upstream, rib-tip and downstream regions were taken arbitrarily along the X-direction at 0.4, 6.6, and 10.4 mm from the reference

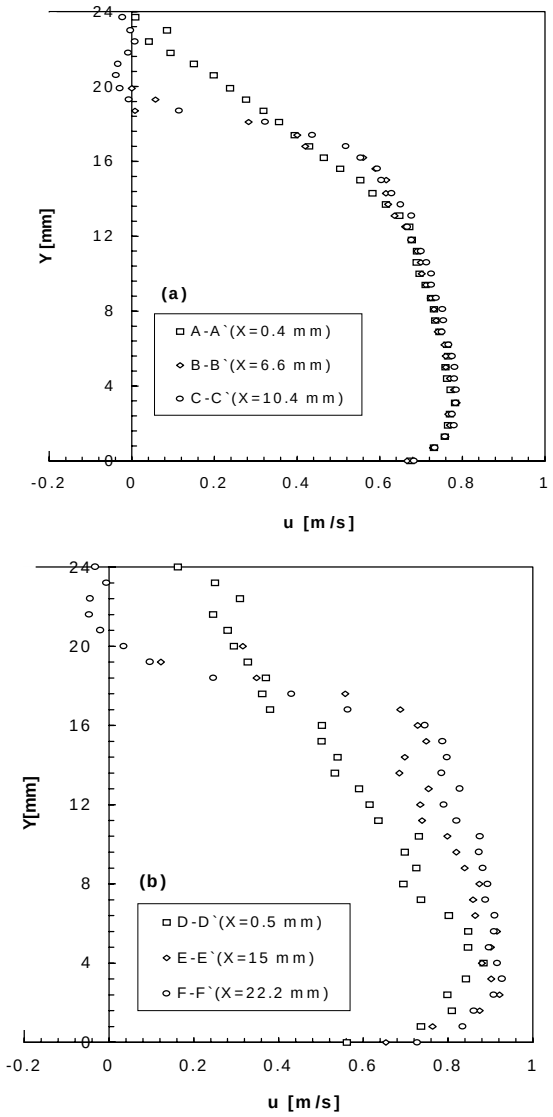

Fig. 9 Streamwise velocity profiles at Re = 20,000
(a) p/k = 10 (b) p/k = 20

point for p/k = 10 while 0.5, 15, and 22.2 mm for p/k=20. The eccentric-parabolic velocity distribution was formed due to roughness effect, which ultimately affected the development of boundary layers. The velocity distribution also showed the back step flows in the downstream regions of the rib. This is obvious due to the separated shear layer within separating and or reattaching flows. The velocity gradient was steeper

over the rib-tip than the upstream and downstream regions. **Figs. 10** and **11** show the calculated turbulent kinetic energy distribution by combining the two components of rms velocity over the same cross-sections of the flow channel at Re = 7,000 and 20,000, respectively. The results showed that the local turbulent kinetic

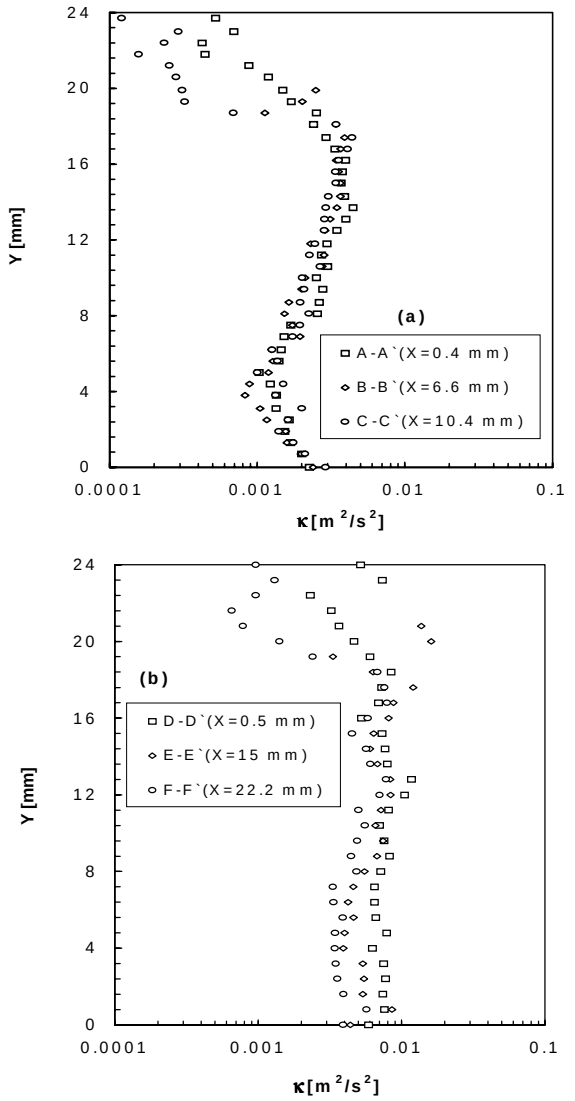

Fig. 10 Streamwise turbulent kinetic energy profiles at Re = 7,000 (a) p/k = 10 (b) p/k = 20

energy has a peak value in front of the ribs whereas its value does not vary enough near the smooth wall. The local turbulent kinetic energy in front of the ribs at p/k = 10 was 40% and 20%lower than that of the p/k =20 for Re =7,000 and 20,000, respectively. This is because; large pitch causes the increase of local turbulent kinetic energy, which yields an increase in the turbulent intensity and accordingly, an increase in both the eddy viscosity and diffusivity of the flow. However, the small pitch causes the increase of acceleration region rather than that of the local turbulent intensity. If the acceleration and the turbulence are combined properly with each other by changing the pitch, the optimum pitch of roughness elements for the augmentation of heat transfer can be found. **Fig. 12** shows the dependency of the reattachment length on the Re. The results showed that the reattachment length depends slightly on the flow conditions and the roughness geometry until reaching Re

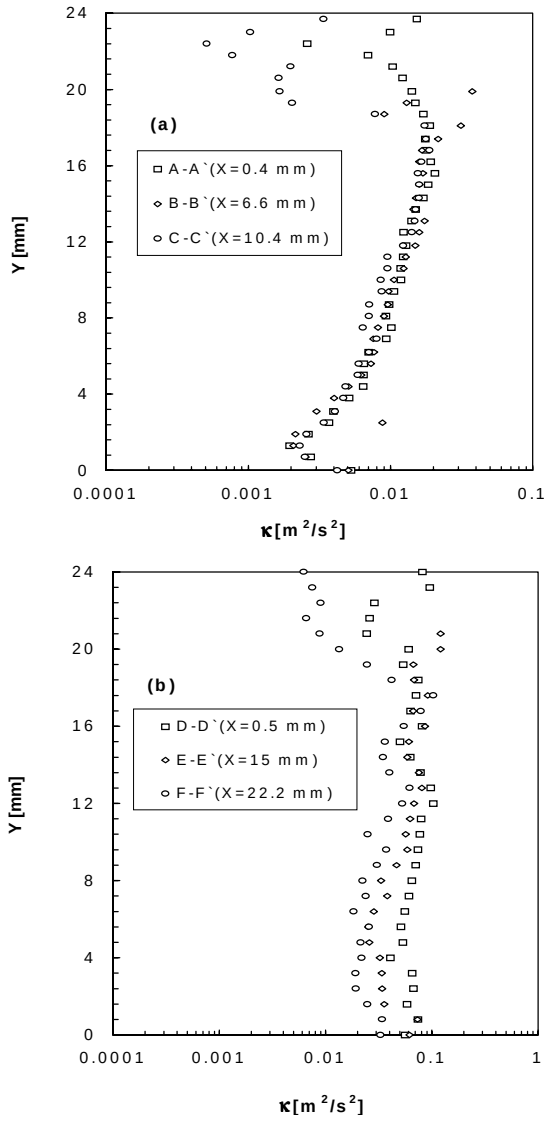

Fig. 11 Streamwise turbulent kinetic energy profiles at Re = 20,000 (a) p/k = 10 (b) p/k = 20

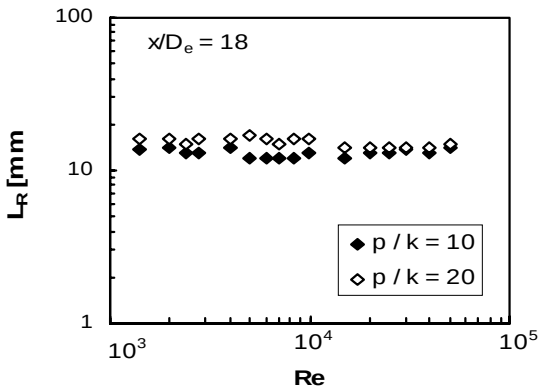

Fig. 12 Dependency of reattachment length on Reynolds number

= 15,000. The reattachment length is almost 4 times the rib height for both the p/k = 10 and 20 within the range of Re investigated, which slightly differs quantitatively from that reported by Mantle (1966) and Faramarzi et al.(1990).The reasons have been claimed due to discrepancy of not only both fluid and flow properties between water and air but also scaling effect of roughness geometry. In addition, there was an uncertainty in both the velocity and the reattachment length measurements, which is to be expected within the range of acceptability. It can be concluded here that the reattachment length depends slightly on the Re and the roughness geometry up to a critical value. The critical value of Re is 15,000 for both the p/k =10 and 20. Beyond this critical value, it is independent of the Re and the roughness geometry in the highly developed turbulent water flows for square cross-sectional ribs (w/k =1).

4.CONCLUDING REMARKS

The main conclusions drawn from the present PIV study are that the recirculations, separations, and turbulent eddies were detected downstream of the ribs. The higher level of turbulent kinetic energy was predicted in front of the ribs and a second peak would be expected upstream of the flow reattachment until encountering the next rib. The flatter velocity profiles in front of the ribs created strong turbulence. The reattachment length is approximately 4 times the rib height for both the p/k ratios of 10 and 20 with the square ribs that were calculated from the velocity vector map for the Reynolds number ranging of 1,400 to 50,000.The reattachment length is independent of the Reynolds number in the highly turbulent flow regime (Re >15,000) while it depends slightly on the Re within the Re range of 1,400 to 15,000 for both the rib geometries. These trends can be treated within the range of acceptable uncertainty. The results can be used as a reference data for the modeling of turbulent flow field over micro-repeated ribs in a narrow channel. However, a detailed investigation of turbulent water flow structures may provide useful information for the efficient design of micro-repeated-rib roughened narrow rectangular channel. Therefore, it is of great importance to optimize the rib geometry in order to find the best augmentation conditions. This, in fact, is what the authors intended to do in the forthcoming future work.

REFERENCES

Acharya, S., et al. “Turbulent Flow Past a Surface-Mounted Two-Dimensional Rib”, Trans. of ASME Vol.116, pp.238-246 (1994).

Bradshaw, P., and Wong, F.Y.F. “The Reattachment and Relaxation of a Turbulent Shear Layer”, J. Fluid Mech., Vol. 52, pp. 113-135 (1972).

Bergeles, G., and Athanassiadis, N. “The Flow Past a Surface-Mounted Obstacle”, J. of Fluids Engineering, Vol. 105, pp.461-463 (1983).

Chang, B.H., and Mills, A.F. “Turbulent Flow in a Channel with Transverse Rib Heat Transfer Augmentation”, Int. J. Heat Mass Transfer, Vol. 36, pp.1459-1469 (1993).

Durst, F., and Rastogi, A. K. “Theoretical and Experimental Investigation of Turbulence Flows with Separation”, Turbulent Shear flows II, Springer Verlag (1980).

Faramarzi, J., and Logan, E. “Reattachment Length Behind a Single Roughness Element in Turbulent Pipe Flow”, Trans. of ASME, Vol.113, pp. 712-714 (1991).

Logan, E., and Phataraphruk, P. “Mean Flow Downstream of Two-Dimensional Roughness Elements” J. of Fluids Engineering, Vol. 111, pp.149-153 (1989).

Lee, C.K., and Abdel-Moneim, S.A. “Computational Analysis of Heat Transfer in Turbulent Flow Past a Horizontal Surface with Two-Dimensional Ribs”, Int. Comm. Heat Mass Transfer, Vol.28, No.2, pp.161-170 (2001).

Mantle, P.L. “A New Type of Roughened Heat Transfer Surface Selected by Flow visualization Techniques”, Proc. Third Int. Heat-Transfer Conf., Vol.1, pp.45-55 (1966).

Shafiqul, I., et. al. “Experimental Study on Heat Transfer Augmentation for High Heat Flux Removal in Rib-Roughened Narrow Channel”, J. of Nuclear Science and Technology, Vol. 35, No.9, pp.671-678 (1998).